PNAS
www.pnas.org

Supplementary Information for

cTAGE5/MEA6 Plays A Critical Role in Neuronal Cellular Components Trafficking and Brain Development

Feng Zhang, Yaqing Wang, Tao Wang, Li Yao, Sin Man Lam, Xiahe Huang, Junwan Fan1, Qin Wang, Liang Liu, Yisheng Jiang, Hongsheng Zhang, Lei Shi, Mei Yu, Guanghou Shui, Yingchun Wang, Fei Gao, Xiaohui Zhang, Zhiheng Xu

Zhiheng Xu
Email: zhxu@genetics.ac.cn

This PDF file includes:

Supplementary Methods and Materials
Figs. S1 to S14
Tables S1 to S2
References for SI reference citations

Other supplementary materials for this manuscript include the following:

None

www.pnas.org/cgi/doi/10.1073/pnas.1804083115

Supplemental Methods and Materials

Image Acquisition and Digitalization of Data

The images related with neuronal morphology, cell number and colocalization were all acquired through Zeiss LSM700 confocal microscopy. In general, the objectives used for these figures were 10*, 20*, 40* and 100*, depending on the resolution needed, and the corresponding Z intervals were 8.0, 3.0, 2.0 and 0.5 μm, respectively. Besides, the parameters for acquisition of each figure, including objective used, the thickness of the z-stack and the number of z-stack, were shown below.

Figures	Objective	Thickness of Z-stack (μm)	No. of Z stacks
Fig 1B	100	4.07	6
Fig 2C	20	9.88	4
Fig 2D	100	0	1
Fig 3A	20	58.4	20
Fig 3D	100	8.1	28
Fig 3E	100	12.9	44
Fig 4A	100	1.5	4
Fig 4B	100	1.5	4
Fig 4D	100	1.5	4
Fig 4F	100	2.5	6
Fig 5A	100	3.5	8
Fig 5B	20	10.12	4
Fig 5F	100	1.85	5
Fig 5G	40	8.35	5
Fig 5H	100	2	5
Fig 6B	100	1.85	5
Fig 6C	100	1.94	5
SFig 1C	100	4.02	7
SFig 4C	100	0	1
SFig 5C	20	6.61	3
SFig 5G	10	32	5
SFig 6A	10	16	3
SFig 6C	10	30	4
SFig 7A	20	64.55	22
SFig 7C	40	4.5	4
SFig 7E	40	4.17	4
SFig 8C	40	0	1
SFig 9A	100	11.7	40
SFig 9B	100	7.8	27
SFig 13B	20	13.22	5

Parameters used for each figure

We used the Imaris software to digitize the data of cell counting, dendrites and spines. For the cell counting like in Fig S6, we employed the “Cell” function in the Imaris software and manually clicked dots on cells which were positive for NeuN, PV or GFAP staining (shown in the figures below), because automatic identification of cells with positive signals through the “Cell” function of the software was not accurate enough. The cell density was defined as the number of cells with positive staining signal in the analyzedregions divided by the area of the analyzed region.

For the digitization of dendrites and spines, the “Filament” function of Imaris software was used according to its manufactory protocol. In brief, for the tracing of dendrites, after Dendrite Beginning Point was clicked on the soma of the analyzed neuron, all the dendrites originating from this soma were carefully traced to their distal ends and the Dendrite Terminal Points were clicked on all these distal ends of dendrites. During this process, the observation was from 360-degree in the 3D view to comprehensively trace the continuous branches originating the soma and find their corresponding distal ends, and exclude the dendrites of other neurons which did not continuously connected to dendrites projecting from the analyzed soma in the 3D view. Then the software would automatically trace the dendrite branches between the Dendrite Beginning Point and all Dendrite Terminal Points, and after manually trimming and revising those tracing filaments that did not match the dendrites very well, the total length of filaments and number of dendrite branch points would be automatically calculated by the “Filament” function of the software. For simulating the spines through the “Filament” function of Imaris software, the Dendrite Beginning Point and Terminal Point were respectively clicked on the both ends of the analyzed dendrite to trace this dendrite. Then the Spine Terminal Points were manually clicked on each distal tip of spines through the 360-degree observation in the 3D view, and all the spines would be automatically identified by the software. After manually trimming and revising the unmatched spines, the spine density along the analyzed dendrite would be calculated by the software.

For the colocalization analysis like in Figure 6B & C, the fixed WT and cKO primary neurons were incubated in the same primary antibody and secondary antibody at the same time, and the confocal images were acquired with the same parameters (like the objective used, thickness of the Z stack and laser intensity). Then we used the “Surface” function of Imaris software to simulate the 3D distribution pattern of Protein X according to its manufactory protocol (shown in figures below). Then the signal intensity of Protein Y distributed inside the simulated Protein X “surface” was calculated by the software, and the relative level of Protein X colocalized with Protein Y was defined as the percentage of intensity of Protein Y distributed in the simulated Protein X “surface” among that of total Protein Y.

We used the ImageJ software to digitalize the staining intensity of some proteins. For SEC31a in Fig.5A, fixed WT and cKO primary neurons were immunostained with the same primary antibody and secondary antibody at the same time, and the confocal images were taken with the same parameters (like the objective used, thickness of the Z stack and laser intensity). Then the images with multiple z-stacks were merged into one z-stack with projection type as Max Intensity. After adjusting the brightness and contrast with the same parameters, the soma of a neuron was selected, and the intensity of the corresponding channel calculated by the “Measure” button was regarded as the staining intensity of SEC31a of that neuron. The staining intensity of SEC31a of all WT and cKO neurons in one batch were normalized to the mean of that of all WT neurons in the same batch.

Primary neuron culture and transfection

The cerebral cortex of the mouse brain at around embryonic 15.5 days (E15.5) was dissected and digested with 0.25% (W/V) Trypsin-EDTA (GIBCO) for 5-10 minutes, and the single-cell suspensions were prepared. For the primary neuron culture, suspended cells (1*105 /mL) were plated into 24-well dishes with pre-coated by poly-D-Lysine (100 μg/mL, Sigma) at room temperature (RT) for 1 hour and cultured in Neurobasal medium

(GIBCO)/B27 supplement (2%, GIBCO)/Glutamax (1%, GIBCO)/Penicillin/Streptomycin (P/S, 1%, GIBCO) at 37℃. For the neurosphere culture, suspended cells (3*104-1*105 /mL) were plated into dishes without pre-coated by poly-D-Lysine and cultured in DMEM/F12 medium (GIBCO)/B27 supplement (2%)/bFGF (20 ng/mL, R & D)/EGF (20 ng/mL, R & D)/P/S (1%). For passage of neurospheres, neurospheres are digested with accutase (Millipore) at RT for 5 minutes. Plasmids were transfected into the primary neurons at 8 days in vitro (div) with Lipofectamine 2000 (Invitrogen).

Infection of GFP-VSVG and Data Analysis

For the image acquisition of the figures shown in Figure 4B-E, primary neurons dissected from around E15.5 WT and cKO cerebral cortex were cultured in the media containing Neurobasal medium/B27(2%)/Glutamax (1%)/ P/S (1%) at 37℃ for 9 days. After insfected with adenovirus-expressing GFP-ts045-VSVG, these cells were cultured in 40, 32 or 37℃ for indicated time. Then, after fixed with 4% PFA at room temperature, WT and cKO primary neurons were incubated in the same primary antibodies (GFP, GM130 and MAP2) and secondary antibodies at the same time, and the confocal images were acquired with the same parameters, including the objective used, thickness of the Z stack and laser intensity. Then we used the “Surface” function of Imaris software to simulate the 3D distribution of GM130 (a marker of Golgi) according to its manufactory protocol. The total volume of GM130 “surface” and the number of fragments of GM130 “surface” were regarded as the volume of Golgi and the number of Golgi fragments, respectively. Besides, the signal intensity of GFP-VSVG distributed in the simulated GM130 “surface” and total GFP-VSVG in the soma was measured by the software, and the percentage of GFP-VSVG localized in Golgi was defined as the percentage of the signal intensity of GFP-VSVG distributed in the simulated GM130 “surface” among that of total GFP-VSVG.

Cortical slice preparation and in vitro electrophysiological recording

The protocols for cortical slice preparation and in vitro electrophysiological recording were performed as described previously with some slight modifications (1). In brief, brain slices (300 μm) of primary motor cortex were prepared from WT or cKO mice at P17-P23. The whole brain were quickly dissected and cut with a vibratome (VT2000, Leica) and then incubated in the artificial cerebrospinal fluid (aCSF, 125 mM NaCl, 2 mM $MgSO_4$, 1.25 mM NaH2PO_4, 1.3 mM Sodium ascorbate, 0.6 mM Sodium pyruvate, 3 mM KCl, 10 mM Glucose, 2 mM CaCl2, 26 mM $NaHCO_3$, 11 mM D-Glucose, and bubbled with 95% O2/5% CO2, pH 7.4) at 34℃ for 30 min, followed by an incubation at 20-22℃ till the electrophysiological recording. The brain slices were transferred into the recording chamber perfused with aCSF solution at 30-32℃ (2 mL/min). For membrane properties recording, whole-cell recording of layer II/III pyramidal cells in the motor cortex of WT and cKO mouse was performed with borosilicate-glass micropipettes (3-5 MΩ), which were perfused with internal solution (143 mM K-gluconate, 7 mM KCl, 10 mM HEPES, 10 mM disodium phopshoscreatine, 4 mM Mg-ATP , 0.3 mM Na-GTP, 0.2 mM EGTA (pH 7.3)) . For mEPSC and mIPSC recording, the borosilicate-glass micropipettes (3-5 MΩ) were filled with normal internal solution(130 mM K+-gluconate, 20 mM KCl, 10 mM HEPES, 0.2 mM EGTA, 4 mM Mg_2ATP, 0.3 mM Na_2GTP, and 10 mM Na_2-phosphocreatine (at pH 7.3, 290–310mOsm)) and high Cl- internal solution (94 mM K+-gluconate, 60 mM KCl, 10 mM

HEPES, 0.2 mM EGTA, 4 mM Mg_2ATP, 0.3 mM Na_2GTP, and 10 mM Na_2-phosphocreatine (at pH 7.3, 290–310 mOsm)). mEPSC were recoded with 1 μM TTX, 20μM CNQX and 50μM AP-5 in the aCSF. mIPSC were recoded with 1 μM TTX, 20μM Bicuculline in the aCSF. The electrical signals were clamped and amplified with a amplifier (Multiclamp 700B, Molecular Devices), followed by digitalized by a digitizer (Digidata 1440, Molecular Devices) at 20 kHz. Then the signals were acquired by Clampex software (V10) and input into a computer for analysis. The recorded neurons were held at -70 mV, recording with the membrane potential (Vm) above -60 mV, access resistance larger than 25 MΩ and input resistant (Rin) changed more than 15% during the recording were discarded.

Lipidomic analysis

Mass spectrometric analyses of lipid profiles in mouse brain tissues were performed on an Agilent HPLC 1260 coupled to Sciex QTRAP 5500 as previously described elsewhere (2-4). For the lipid extraction, four dissected WT and cKO mouse brains at P14 (approximately 30 mg of samples) were freshly frozen in the liquid Nitrogen and the frozen samples were inactivated by 900 μL of chloroform:methanol (1:2) plus with 10% deionized H_2O. After homogenization, the samples were further incubated at 1500 rpm at 4℃ for one hour. Then, 400 μL of deionized H_2O and 300 μL of chloroform were added in the samples to break the phase, and the lower organic phase was collected to a fresh tube. 500 μL of chloroform were added for a second extraction of lipid components, which was pooled into the same tube. The samples were dried with SpeedVac (Genevac, UK) and stored at -80℃ until analysis.

Behavior tests

The behavior tests were performed as described (5). In brief, for tail suspension test, the mice were suspended through their tails, and whether they have the abnormal limb clasping reflexes were observed. The percentage of time for those mice spending in the abnormal limb clasping reflexes during the observation time of 0.5-1 minute was measured. For Rota-Rod test, mice at postnatal 16 days were put on the rotating rod of Rota Rod Treadmills at 10 rpm, and the time of which those mice spent staying on the rotating rod were measured. For open field test, the mice were put into a chamber (40 cm*40 cm*49 cm) with white background, and their movement were observed and analyzed with SMART software. If the speed of a mouse was below 0.3 cm/s, the mouse was thought to be at rest. The moving distance, speed, move duration and rest duration of those mice in the observation time of 1800 s were measured.

Supplemental Figure 1

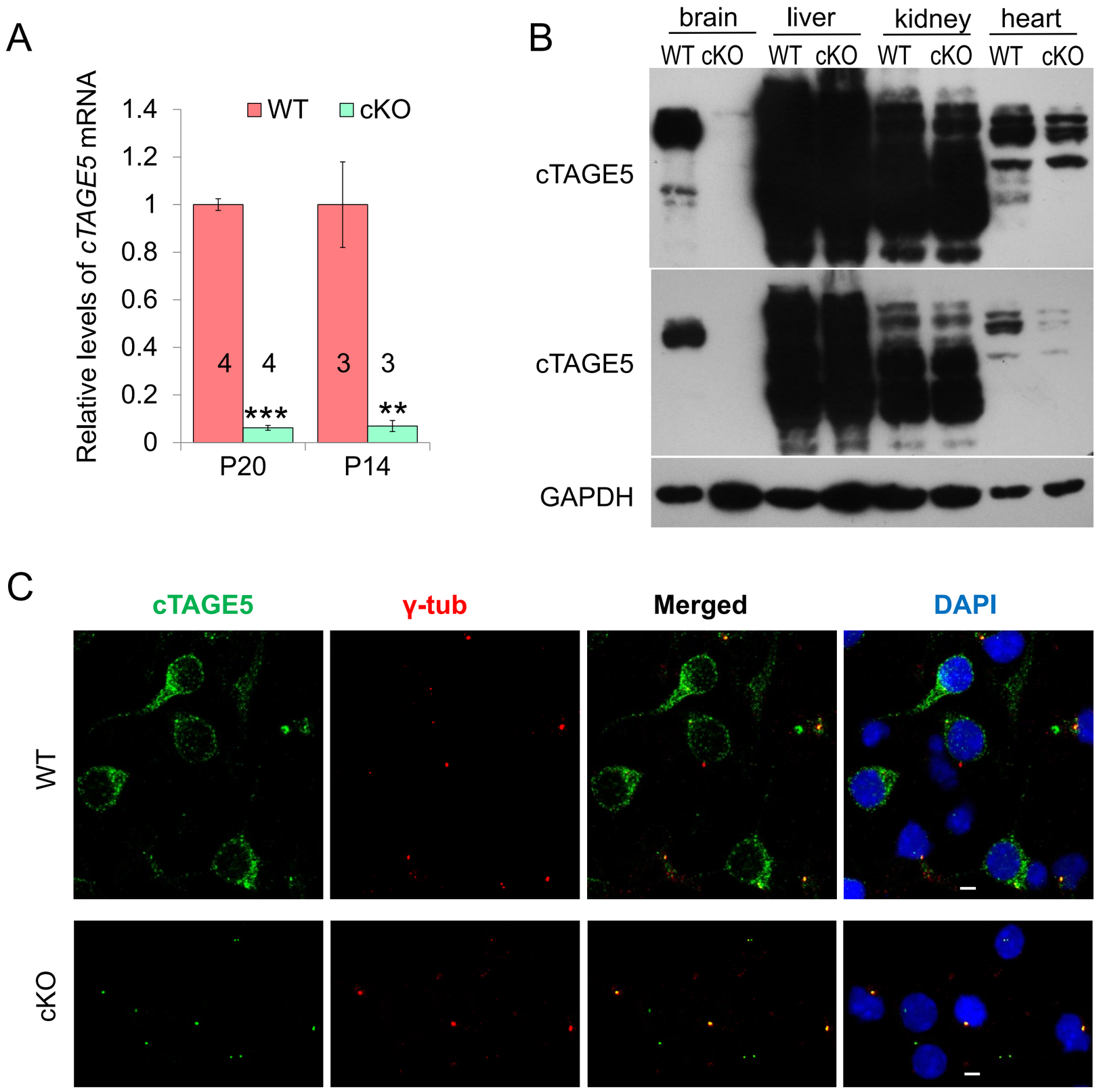

Supplemental Figure 1. *cTAGE5* was specifically knocked out in the brain of Nestin Cre-cKO mouse

(A). The mRNA levels of *cTAGE5* in the cerebral cortex of WT and cKO mouse at P20 and P14 were determined with Real-time PCR. β-Actin was used as loading control. t-test; ** ($P<0.01$); *** ($P<0.001$). (B). Protein levels of cTAGE5 in the brain, liver, kidney and heart of WT and cKO mice were inspected by Western blotting. Longer exposure time was shown in the upper panel. GAPDH was used as loading control. (C). Primary neurons at 14 div dissected from around E15.5 WT and cKO mouse brains were stained with cTAGE5 and γ-tub antibodies. Bars: 5 μm. Nucleus was stained with DAPI.

Supplemental Figure 2

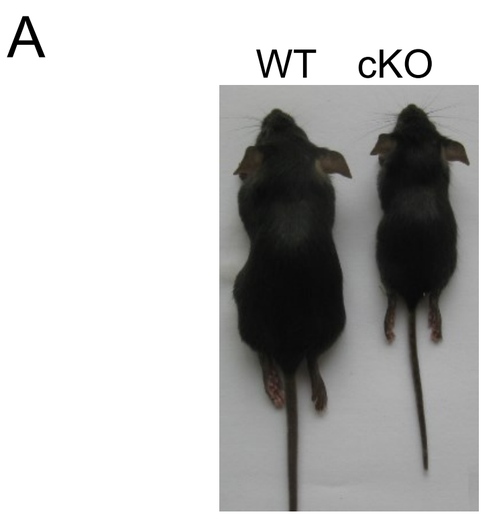

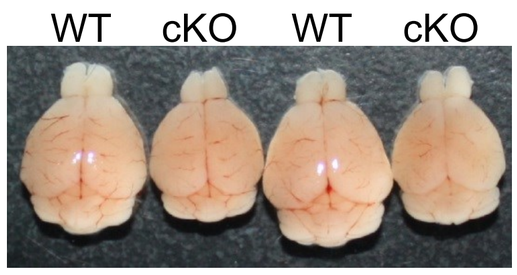

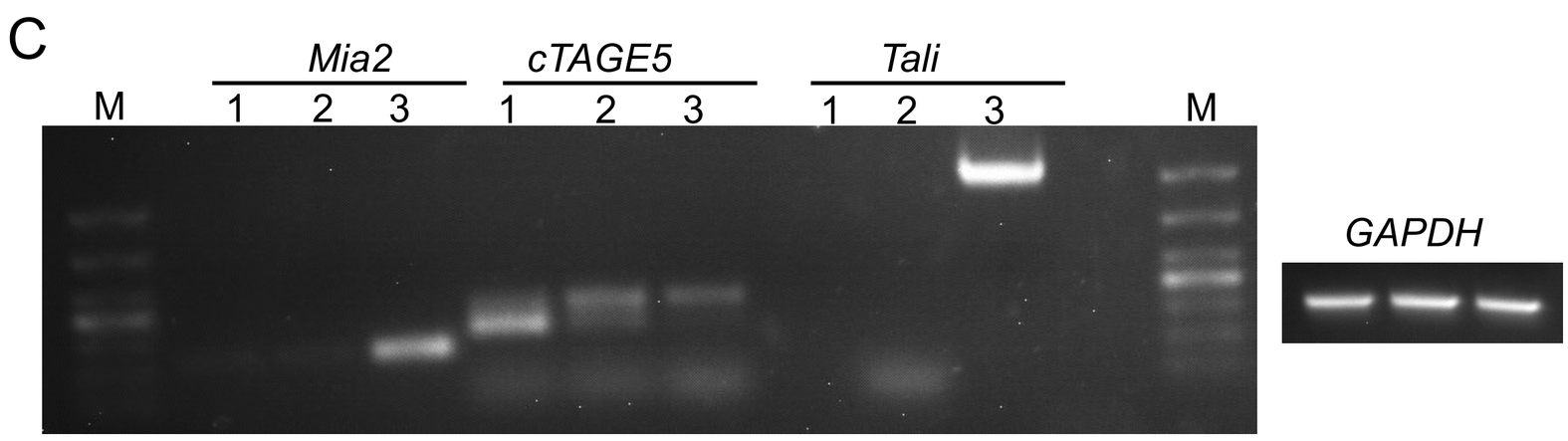

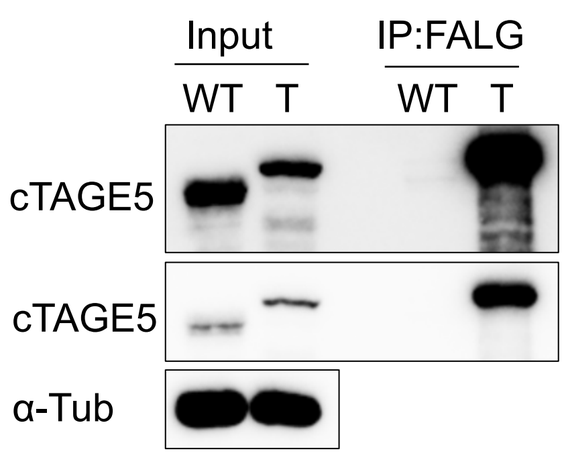

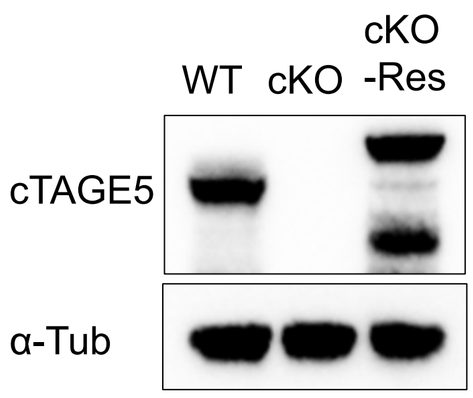

Supplemental Figure 2. The lethality and developmental defects of *cTAGE5* cKO mouse can be rescued by transgenic expression of human *FLAG-cTAGE5*

(A). Images of WT and cKO mice at P20. (B). Images of the brains dissected from WT and cKO mice at P20. (C). The expression pattern of *Mia2*, *cTAGE5* and *Tali* genes in WT and cKO mouse brains and WT mouse pancreas at P20 was determined by reverse transcription PCR. *Tali* hybrid gene was not detected in the brain. 1: WT mouse brain; 2: cKO mouse brain; 3: WT mouse pancreas; M: DNA marker. GAPDH was used as loading control. (D). The expression of endogenous cTAGE5 and FLAG-cTAGE5 in WT and FLAG-cTAGE5 transgenic mouse brains at P16 was determined by Western blotting. The upper panel was over-exposure image. WT: wild-type; T: *FLAG-cTAGE5* transgenic mouse. (E). The expression of endogenous cTAGE5 and FLAG-cTAGE5 in WT, cKO and cKO-Res mouse brains at P20 was determined by Western blotting. α-tubulin was used as loading control.

Supplemental Figure 3

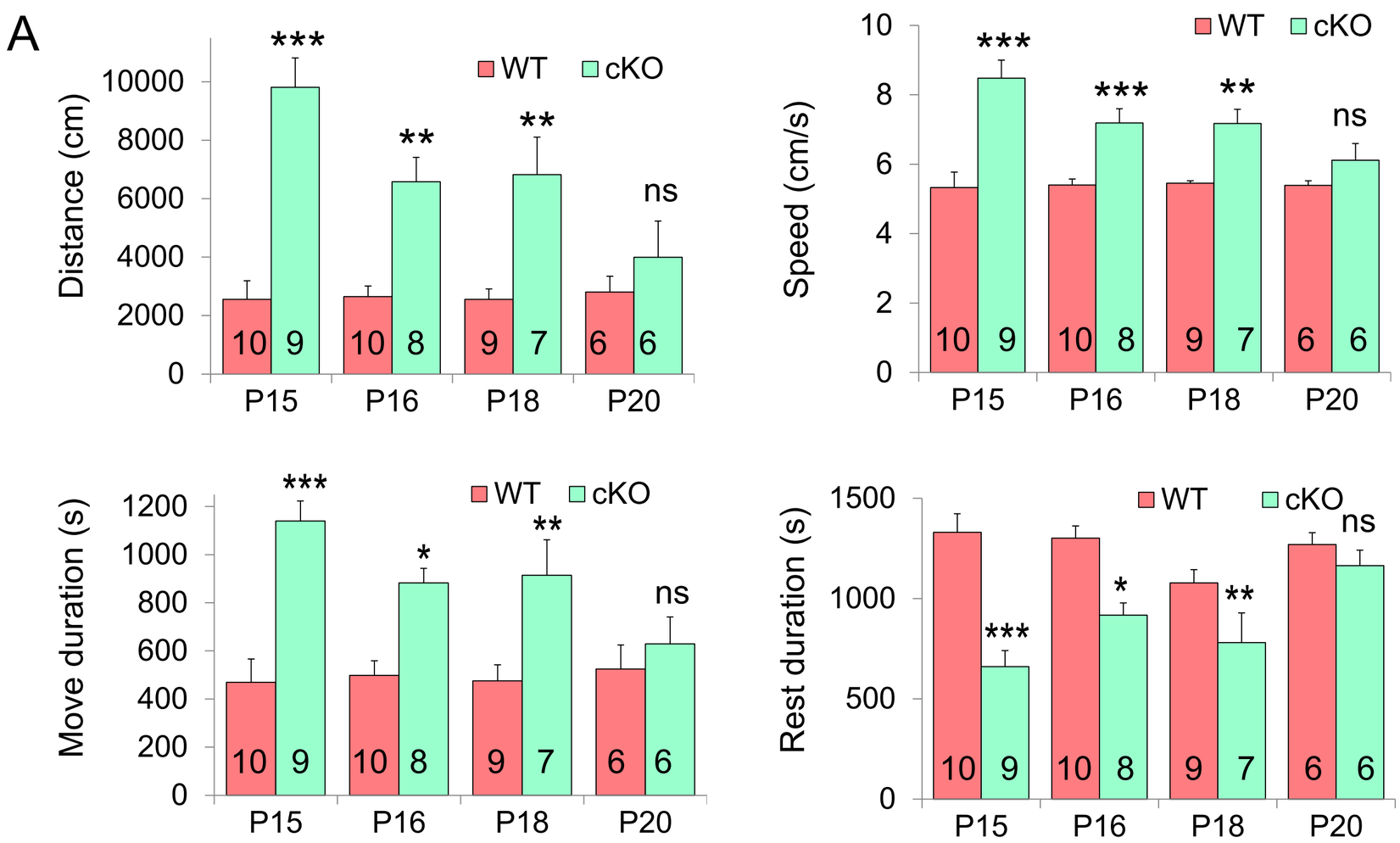

Supplemental Figure 3. The *cTAGE5* cKO mice show higher movement activity in the open-field test

(A). The moving distance, speed, move duration and rest duration of WT and cKO mice at different developmental stages in the open field test were measured. t-test; * (P<0.05), ** (P<0.01), *** (P<0.001), ns (not significant). Numbers of mice tested were labeled in the panels.

Supplemental Figure 4

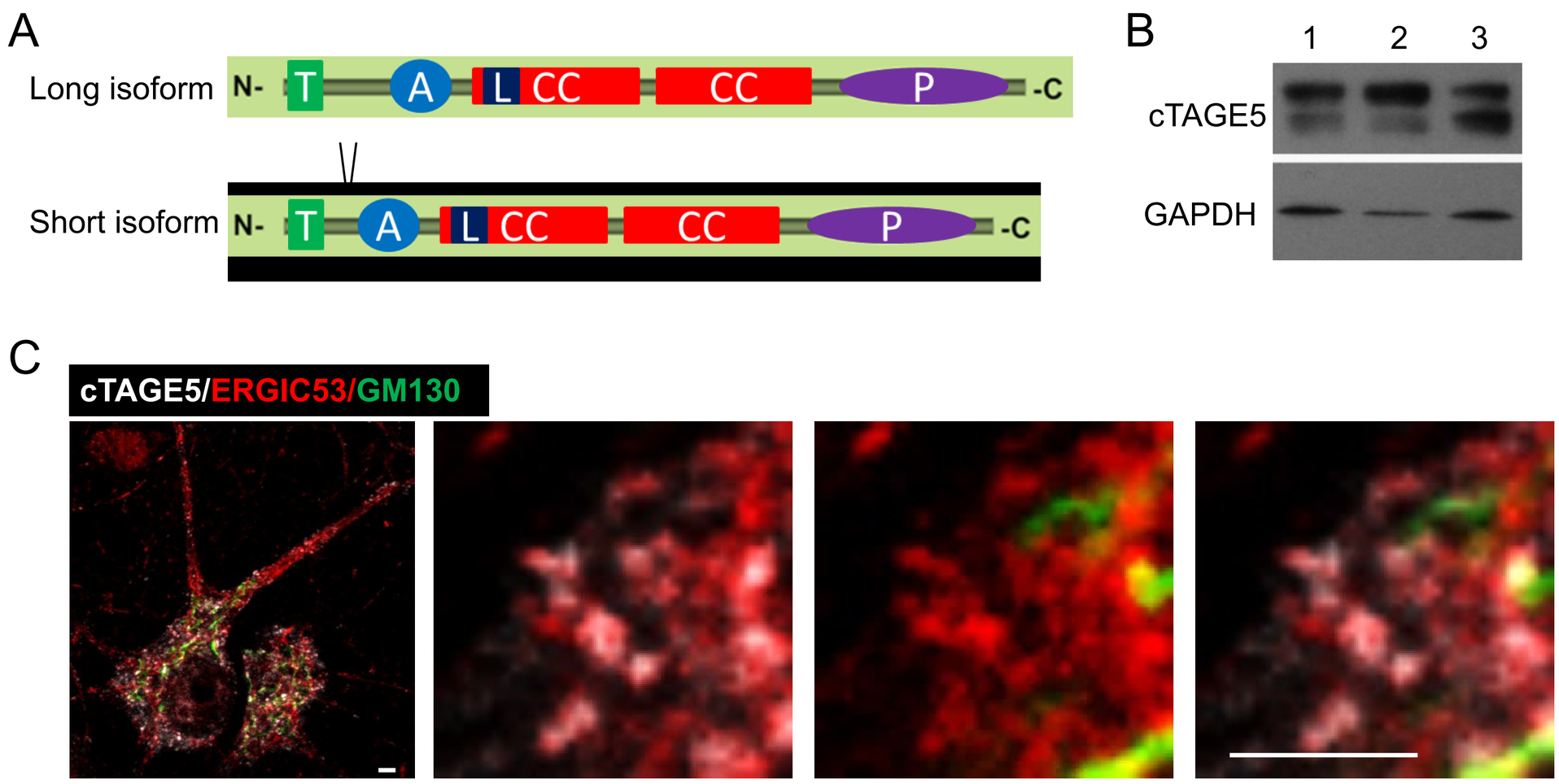

Supplemental Figure 4. cTAGE5 is expressed in mouse brain as a specific shorter splicing isoform in neuron.

(A). Schematic illustration of the structure of cTAGE5, which contains a transmembrane domain (T) in the N terminus, an Acidic activation domain (A), a Heptad Leucine repeat domain (L), two Coiled-coil domains (CC) and a Proline-rich domain (P) in the C terminus. A fragment of 99nt at N-terminus is alternatively spliced to form the short isoform. (B). West blotting result showing that cTAGE5 protein is mainly expressed as a shorter isoform in the embryonic brain, compared with meninges. GAPDH was used as the loading control. 1: E14 meninges; 2: E18 meninges; 3: E14 brain. (C). Primary neurons (14 days *in vitro*, 14 div) dissected from E15.5 wild-type mouse cerebral cortex stained with cTAGE5, ERGIC53 and GM130 antibodies. The cells were fixed with methanol. Bars: 2 μm (C).

Supplemental Figure 5

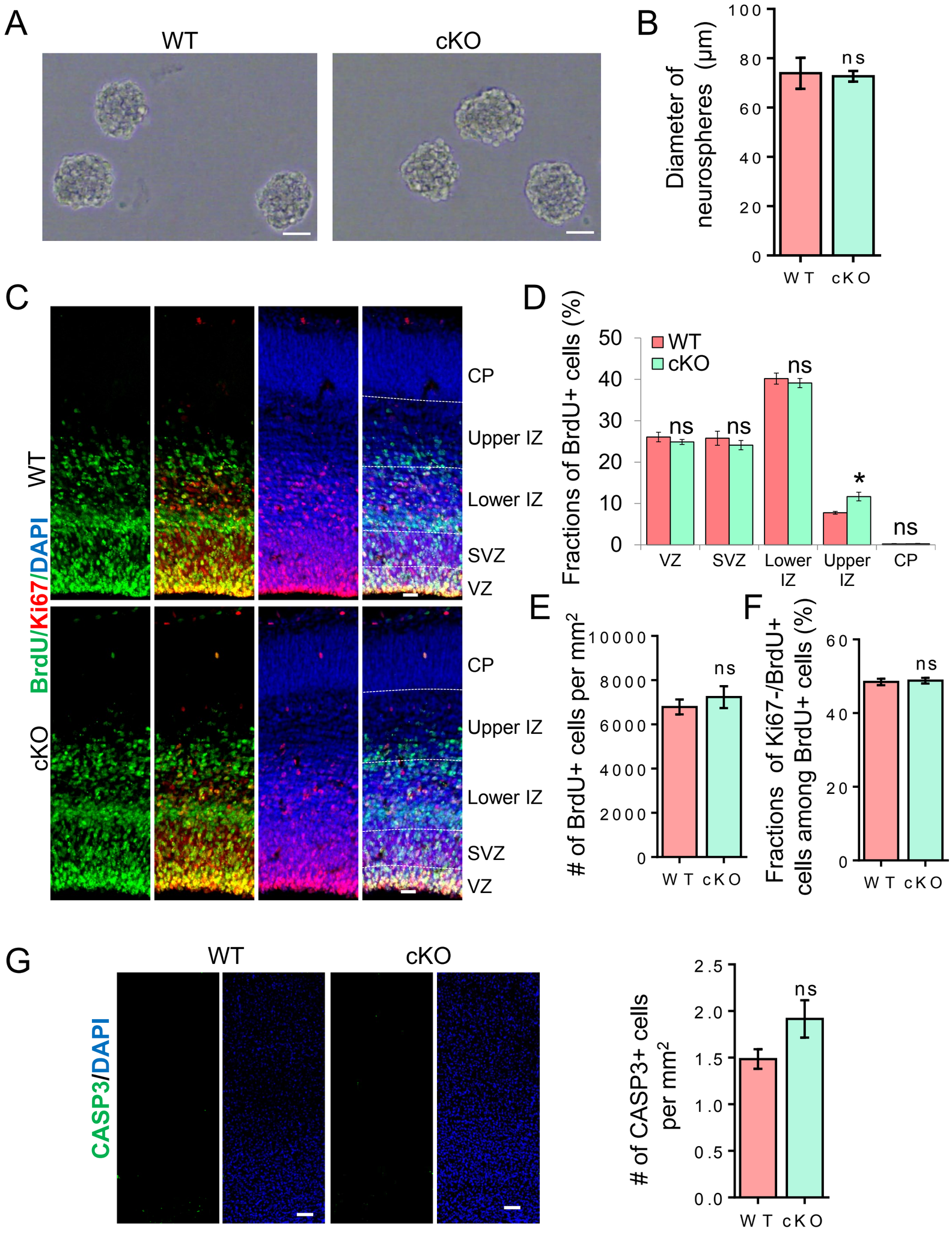

Supplemental Figure 5. *cTAGE5* cKO has no significant effect on the development of neuronal progenitor cell (NPC).

(A-B). The images of neurospheres from the second-generation of NPC dissected from around E15.5 WT and cKO mouse cerebral cortex, and quantification analysis of their diameters. WT: n=254/3; cKO: n=499/3 (# of neurospheres / # of mice). t-test; ns, not significant. (C). Coronal sections of E15.5 wild-type or cKO brain slices labeled with BrdU (100 μg/Kg) at E14.5 and stained with anti-BrdU (green) and Ki67 (red) antibodies. (D). Quantification of $BrdU^+$ cell distribution in the cortex in (C). (E) Quantification analysis of the density of $BrdU^+$ cells in the cortex in (C). (F) Quantification analysis of the fractions of $BrdU^+/Ki67^-$ cells among $BrdU^+$ cells in (C). n=10/3 (# of brain slices / # of mice). t-test; * ($P<0.05$), ns (not significant). (G). Coronal sections of P20 WT or cKO cerebral cortex stained with cleaved-Caspase3 (CASP3) antibody (green) and quantification analysis of apoptotic cell density in the cortex. t-test; ns (not significant). n=7. Bars: 10 μm (A); 25 μm (C); 100 μm (G). Nucleus was stained with DAPI.

Supplemental Figure 6

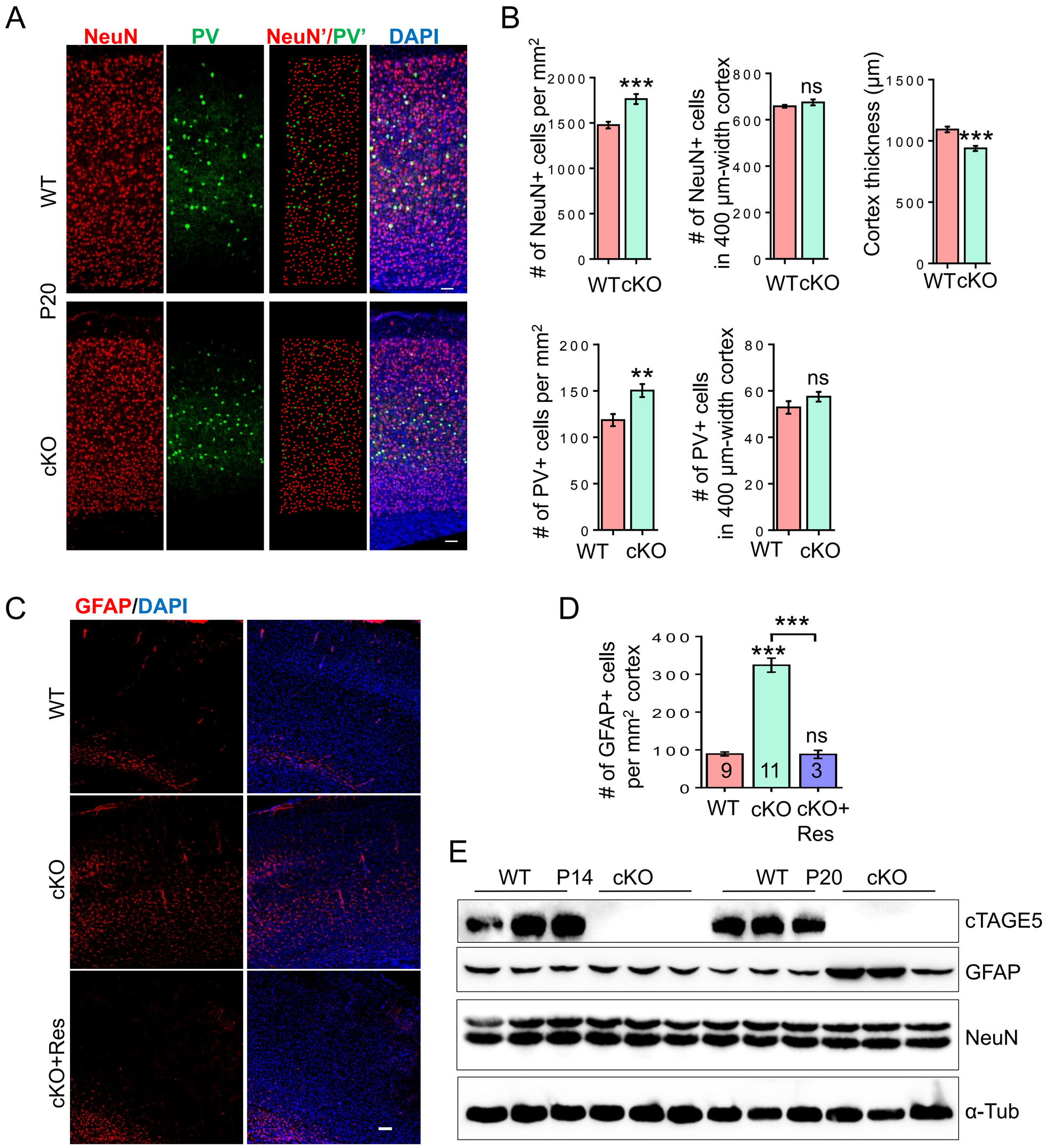

Supplemental Figure 6. cKO of *cTAGE5* leads to increased neuron density and activation of astrocytes in the cerebral cortex

(A). Coronal sections of P20 WT or cKO cerebral cortex stained with NeuN (neuron marker) and parvalbumin (PV, inhibitory neuron marker) antibodies. NeuN'/PV': the simulated NeuN and PV signal by Imaris Software. (B). Quantification of cortical thickness, density and number of $NeuN^+$ neurons, and density and number of PV^+ neurons in (A). t-test; ** ($P < 0.01$), *** ($P < 0.001$), ns (not significant). n=6. (C). Coronal sections of WT, cKO or cKO-Res cerebral cortex at P20 stained with GFAP (astrocyte marker) antibody. (D). Quantification of density of GFAP positive astrocytes in (C). One-way ANOVA; *** ($P < 0.001$), ns (not significant). (E). Western blotting results showing the expression levels of NeuN and GFAP in WT or cKO mouse cerebral cortex at P14 and P20. α-tub was used as loading control. Bars: 50 μm (A); 100 μm (C). Nucleus was stained with DAPI.

Supplemental Figure 7

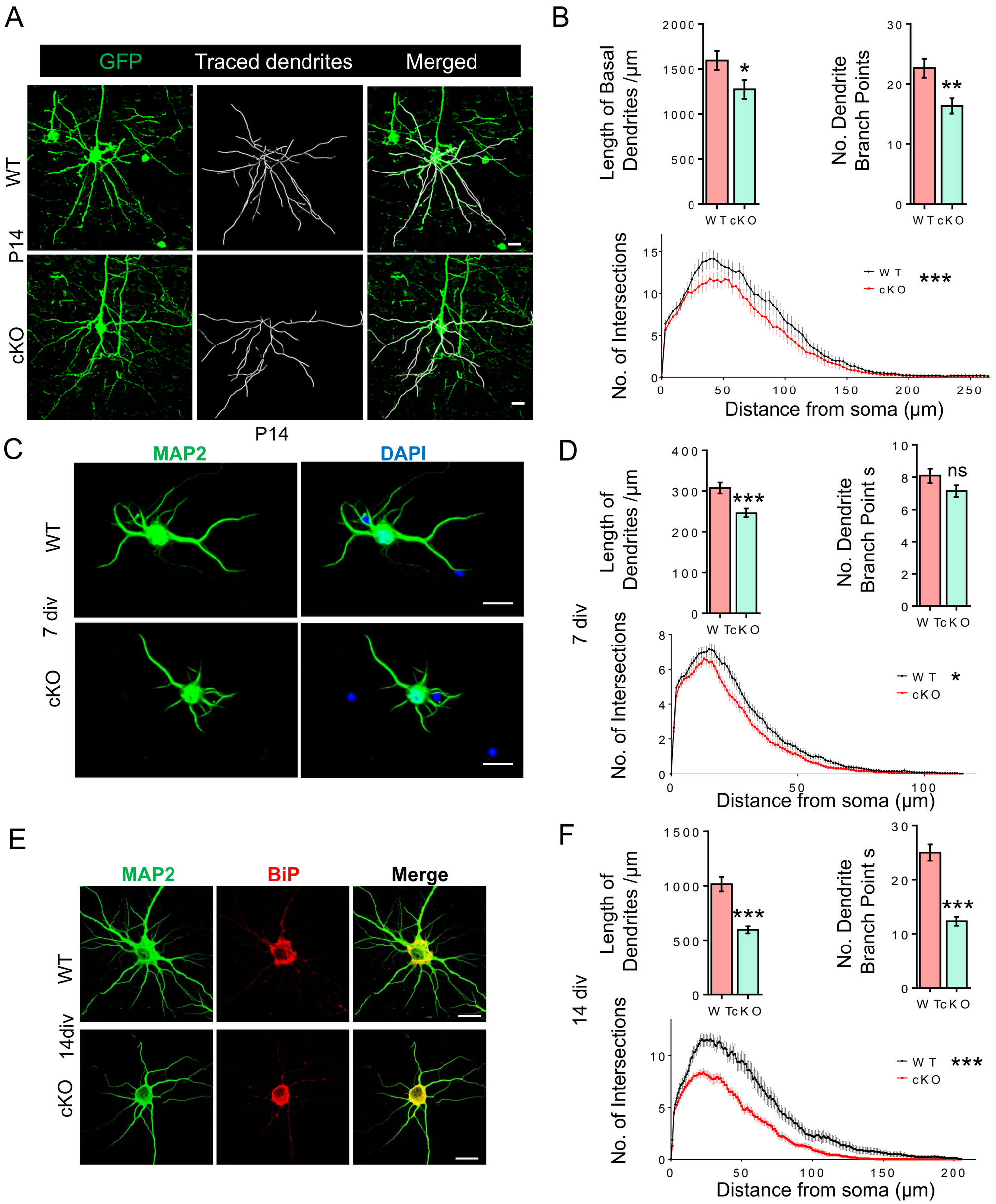

Supplemental Figure 7. cKO of *cTAGE5* leads to defects in dendrites outgrowth of neurons both *in vivo* and *in vitro*.

(A). Representative images of Thy1-*GFPm* labelled pyramidal neurons in the WT or cKO motor cortex at P14. The basal dendrites of pyramidal neurons was reconstructed using the "filament" function of Imaris software. (B). The total length of basal dendrites, the number of basal dendrite branch points and the basal dendritic complexity in (A) was analyzed with Imaris software. t-test (Kolmogorov-Smirnov test for Sholl analysis); * ($P < 0.05$); ** ($P < 0.01$); *** ($P < 0.001$). WT: n=16/5; cKO: n=21/5. (C-F). Representative images of primary neurons at 7 div (in C) and 14 div (in E) dissected from E15.5 WT or cKO brain and stained with MAP2 and/or Bip antibodies. Left panels: the total dendritic length, number of dendrite branch points and the dendritic complexity of primary neurons at 7 div (in C) and 14 div (in E) were analyzed with Imaris software. t-test (Kolmogorov-Smirnov test for Sholl analysis); * ($P < 0.05$); *** ($P < 0.001$); ns: (not significant). 7 div (WT: n=54/4; cKO: n=58/4); 14 div (WT: n=23/4; cKO: n=28/4). (n, # of neurons analyzed / # of mice analyzed). Bars: 20 μm (A, C, E).

Supplemental Figure 8

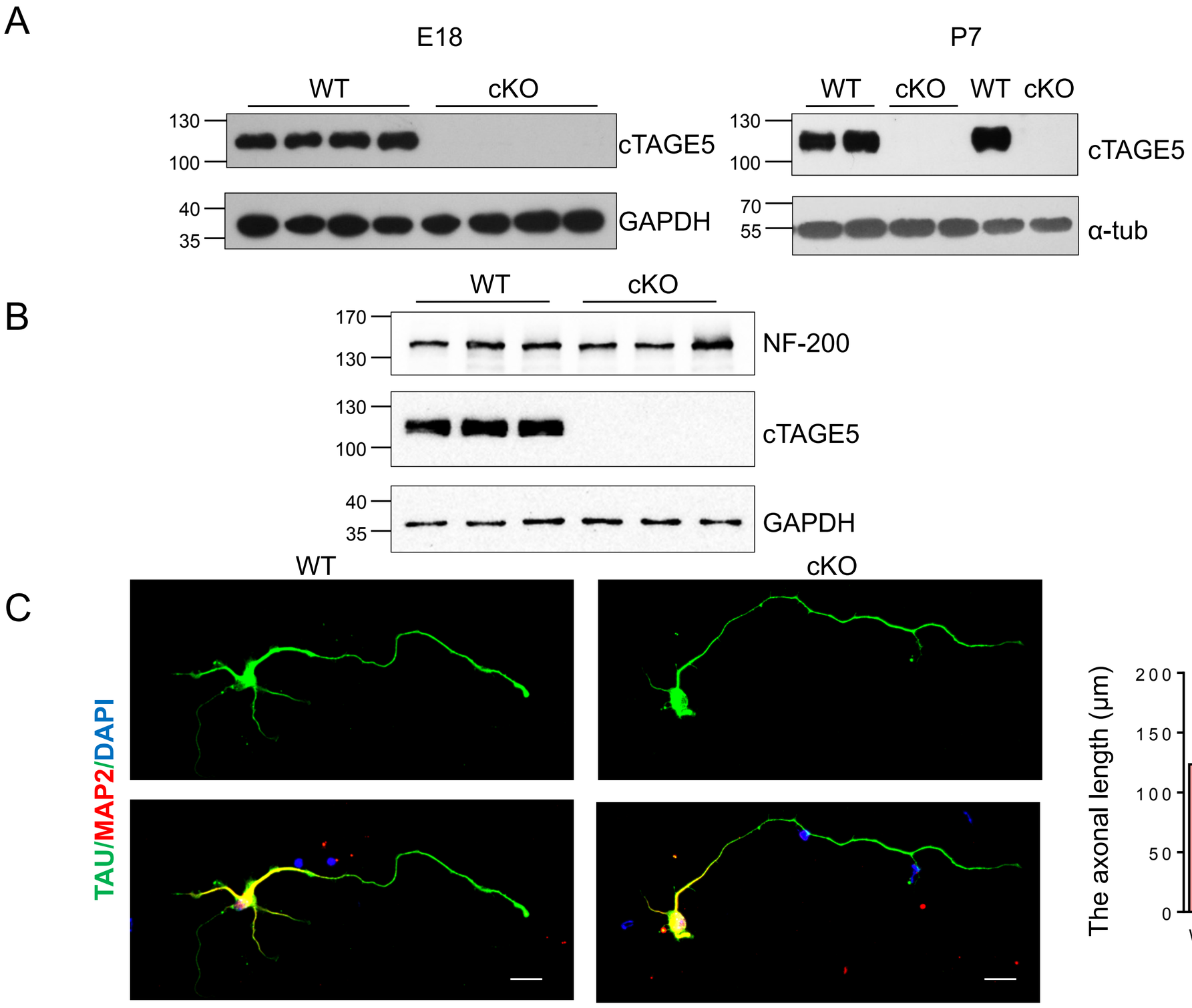

Supplemental Figure 8. *cTAGE5* cKO did not significantly affect the axonal outgrowth.

(A). The protein levels of cTAGE5 in the cerebral cortex of WT and cKO mouse at early developmental stages (E18 and P7) were determined by Western blotting. GAPDH or α-tub were used as loading controls. (B). The protein levels of axonal markers NF-200 in the cerebral cortex of P20 WT and cKO mouse were determined by Western blotting. GAPDH were used as loading controls. Three independent replicates were performed. (C). Representative images of primary neurons at 4 div dissected from E15.5 WT or cKO brain and stained with MAP2 and TAU antibodies. The length of axons indicated by the longest TAU^+ processes were analyzed with Imaris software. t-test; ns (not significant). WT: n=119/4; cKO: n=97/4. (n, # of neurons analyzed / # of mice analyzed). Bars: 20 μm.

Supplemental Figure 9

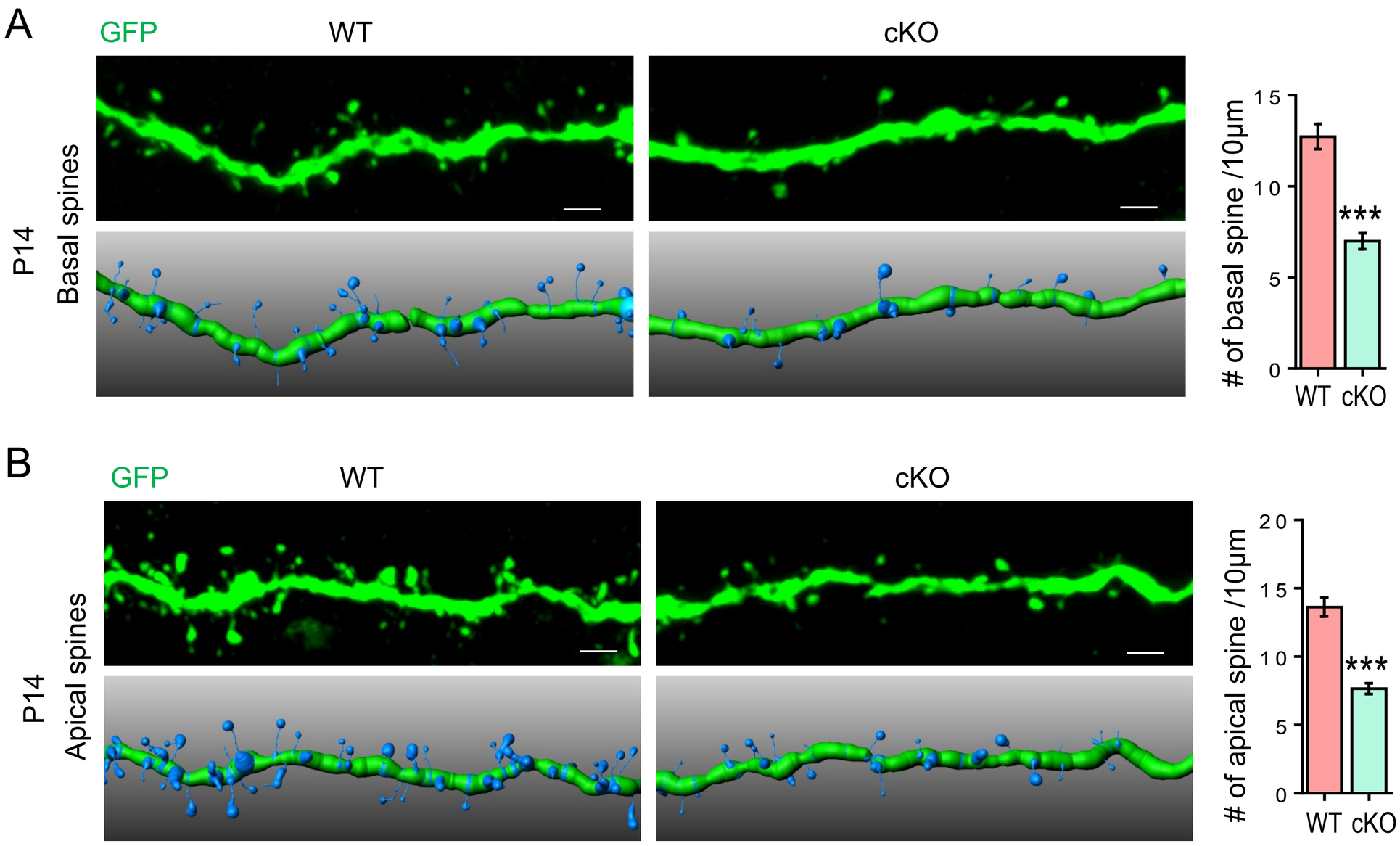

Supplemental Figure 9. *cTAGE5* cKO leads to defects in spine formation in neurons of P14 brains.

(A-B). Representative images of basal (A) and apical (B) dendrites of Thy1-*GFPm* labelled pyramidal neurons in the WT or cKO cerebral cortex at P14. The spine density was defined as the number of spines along 10 μm secondary dendrites and analyzed with the Imaris Software. t-test; *** (P<0.001). Basal (WT: n=25/4; cKO: n=38/4); apical (WT: n=15/4; cKO: n=22/4). (n, # of dendrites analyzed / # of mice analyzed). Bars: 2 μm.

Supplemental Figure 10

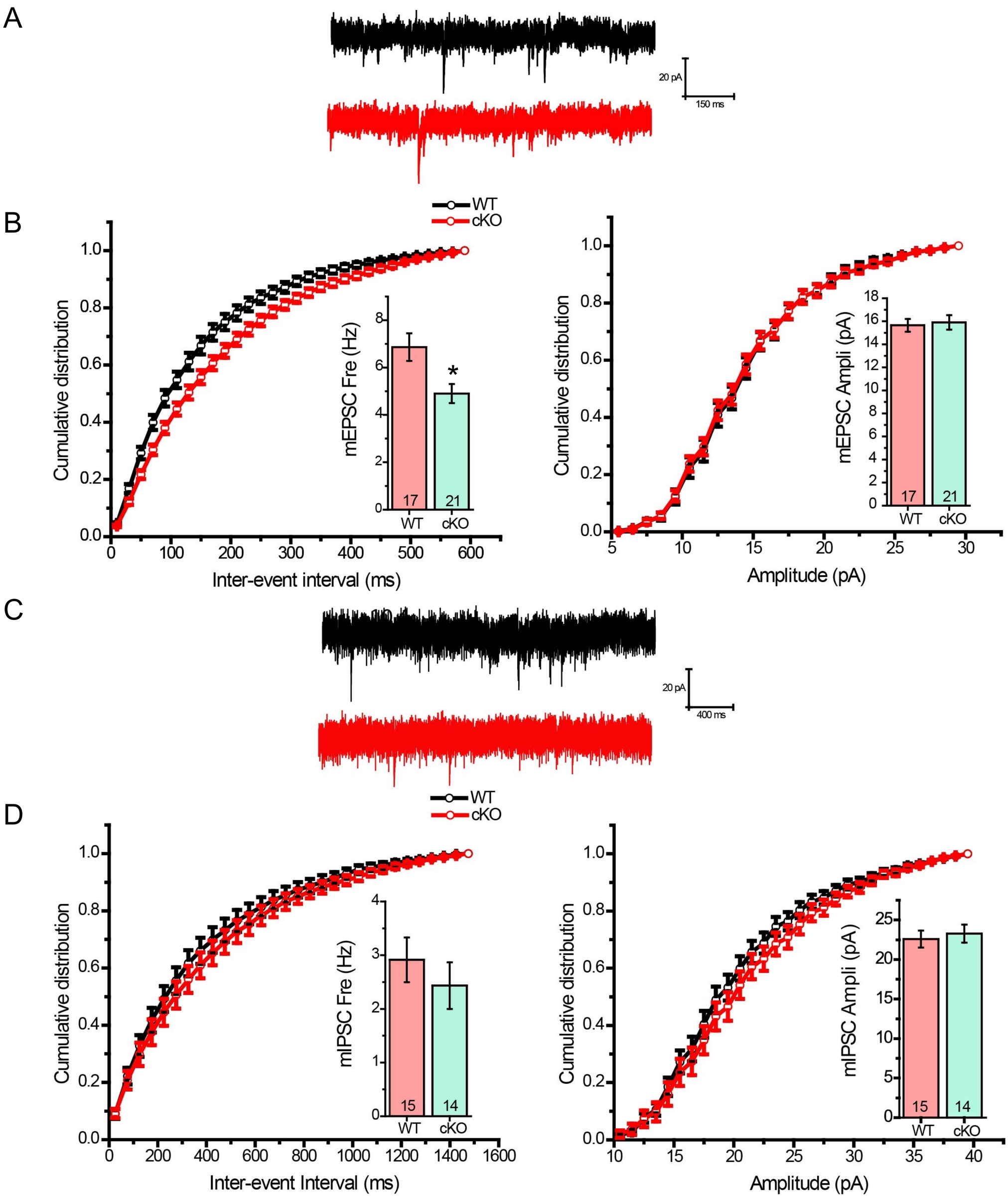

Supplemental Figure 10. mEPSC of LII/III pyramidal cells in motor cortex is decreased in *cTAGE5* cKO mice, whereas mIPSC is not affected.

(A). Sample traces of mEPSC in WT and cKO motor cortex at P17-23. (B). Bar graphs and cumulative distribution of frequency and amplitude of mEPSC recorded from L2/3 pyramidal neurons in motor cortex. Mann-Whitney U test; * $P<0.05$. WT: n=17/3; cKO: n=21/3. (n, # of neurons analyzed / #of mice analyzed).

(C). Sample traces of mIPSC in WT and cKO motor cortex at P17-23. (D). Bar graphs and cumulative distribution of frequency and amplitude of mIPSC recorded from L2/3 pyramidal neurons in motor cortex. Mann-Whitney U test. WT: n=15/3; cKO: n=14/3. (n, # of neurons analyzed / #of mice analyzed).

Supplemental Figure 11

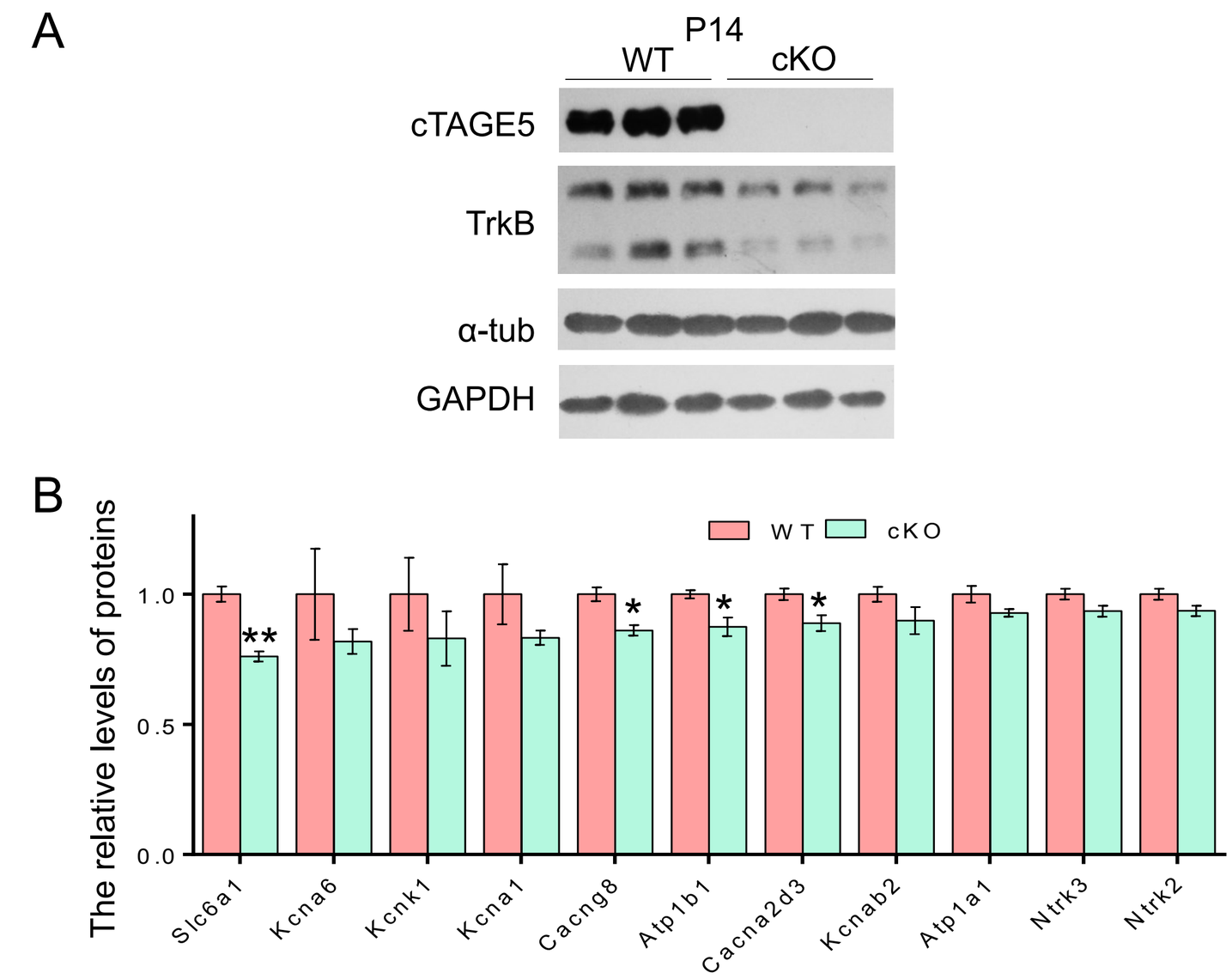

Supplemental Figure 11. *cTAGE5* cKO affects the expression of ion channels and receptors in the brain.

(A). The protein levels of TrkB in the cerebral cortex of P14 WT and cKO mouse were determined by Western blotting. α-tub and GAPDH were used as loading controls. Three independent replicates were performed. (B) The relative protein levels of ion channels and cell receptors in the cerebral cortex of P14 WT and cKO mouse were determined by quantitative mass spectrometry. t-test; * ($P < 0.05$); ** ($P < 0.01$). 3 WT and cKO mice were analyzed.

Supplemental Figure 12

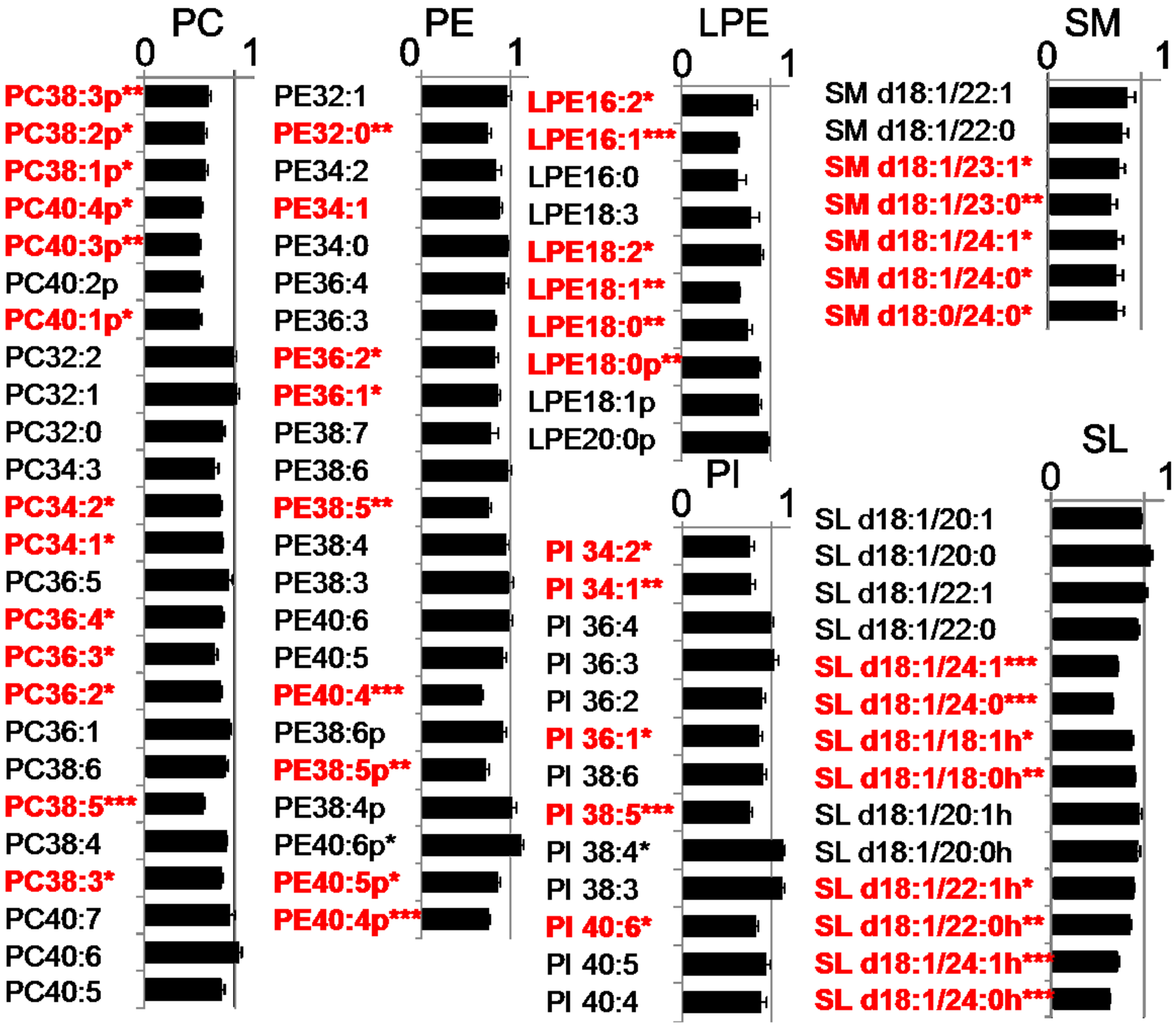

Supplemental Figure 12. *cTAGE5* cKO leads to the down-regulation of lipid levels in the cerebral cortex.

The levels of lipid components in the WT and cKO cerebral cortex at P14 were analyzed by HPLC. PC, phosphatidylcholines; SM, sphingomyelins; PE, phosphatidylethanolamines; LPE, lyso-PE; PI, phosphatidylinositols; SL, sulfatides. t-test; * ($P < 0.05$); ** ($P < 0.01$); *** ($P < 0.001$). n=4.

Supplemental Figure 13

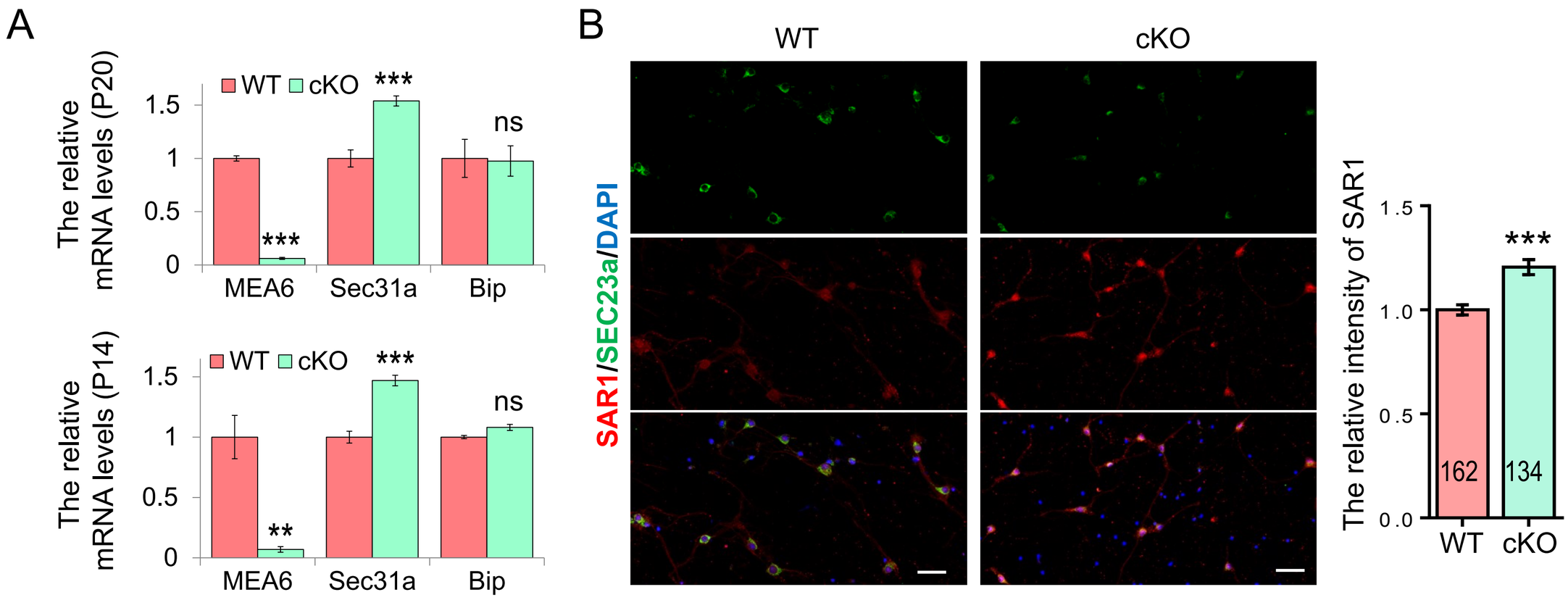

Supplemental Figure 13. Up-regulation of *SEC31a* mRNA level and SAR1 protein level in *cTAGE5* cKO brain.

(A). The mRNA levels of *cTAGE5*, *Sec31a* and *Bip* in the cerebral cortex of WT and cKO mouse at P20 and P14 were determined by Real-time PCR. β-Actin was used as loading control. t-test; ** ($P < 0.01$); *** ($P < 0.001$); ns (not significant). P20 (n=4); P14 (n=3). (B). Primary neurons at 14 div dissected from around E15.5 WT and cKO brains were stained with SAR1 and SEC23a antibodies. Right panels: Quantification of relative staining intensity of SAR1. t-test; *** ($P < 0.001$). 4 WT and cKO mice were analyzed. Bars: 50 μm. Nucleus was stained with DAPI.

Supplemental Figure 14

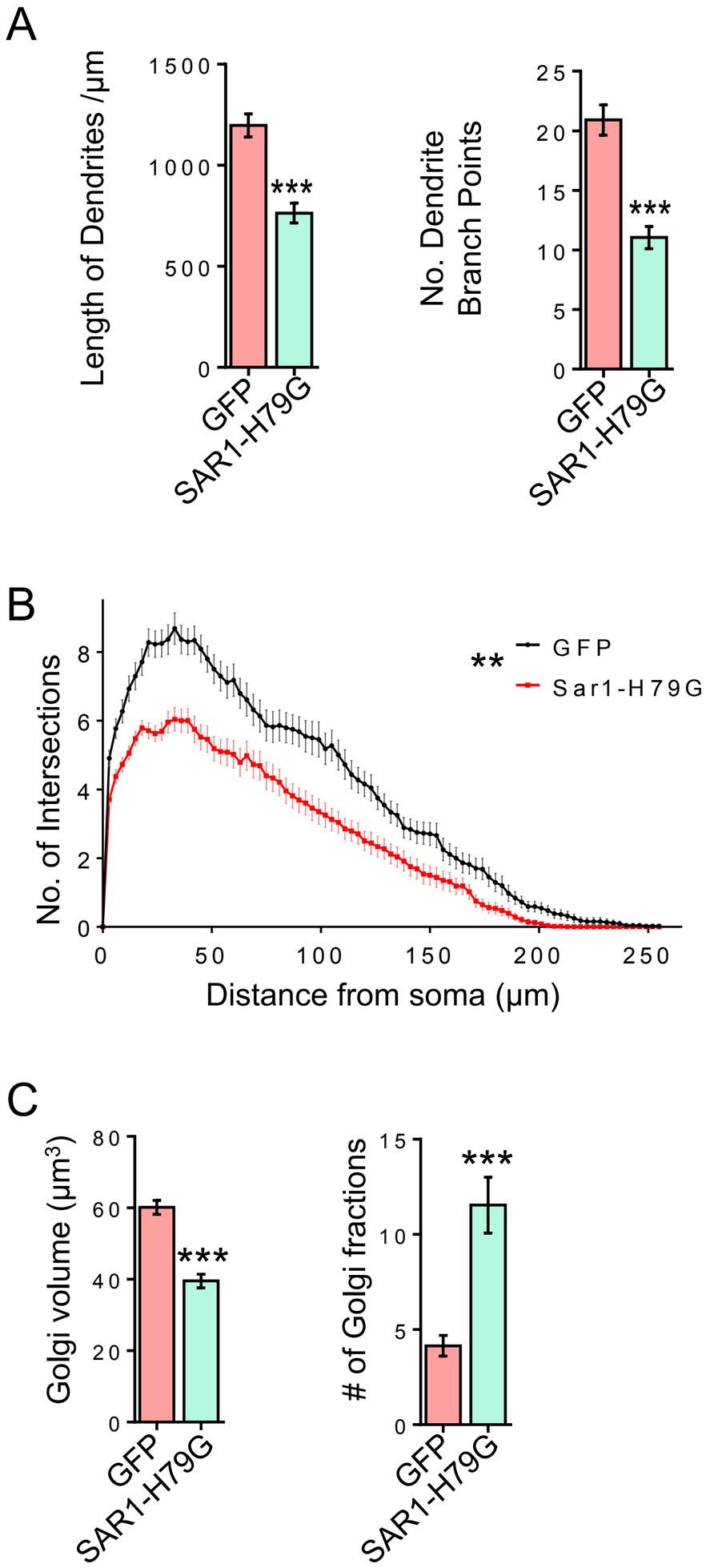

Supplemental Figure 14. Overexpression of SAR1-H79G leads to decreased dendritic complexity and fragmentation of Golgi apparatus in neuron.
(A-B). The dendrites of neurons labelled by GFP and MAP2 in Figure 5G were reconstructed by using the "filament" function of Imaris software, and thus the total dendrite length, the number of dendrite branch points and the dendritic complexity was calculated with Imaris. t-test (Kolmogorov-Smirnov test for Sholl analysis); * ($P<0.05$); ** ($P < 0.01$); *** ($P < 0.001$); GFP: n=44/3; SAR1-H79G: n=48/3. (C) Quantification of Golgi volume and the number of Golgi fractions in neurons labeled by GM130 and GFP in Figure 5H. t-test; *** ($P < 0.001$); GFP: n=47/3; SAR1-H79G: n=50/3. (n, # of neurons analyzed / # of mice analyzed).

Supplemental Table 1

Table S1. The changes of protein expression levels in cKO mouse brains from Quantitative Mass spectrometry analysis.

Proteins	Ranks in changed levels	Expression in WT	Expression in cKO	cKO/WT	P value
LMAN2	3	11825	6935	0.586	0.0001
TRAPPC12	4	2653	1584	0.597	0.2674
CLTB	6	258	168	0.649	0.0183
UBXN8	10	7038	5119	0.727	0.0708
CPLX3	11	6496	4733	0.729	0.0043
COPZ1	16	2142	1630	0.761	0.0029
SLC6A1	17	20372	15512	0.761	0.0025
APOA1	25	30343	23783	0.784	0.0093
PCSK1N	27	11555	9179	0.794	0.0030
KCNA6	37	1725	1411	0.818	0.3729
COPG2	46	6969	5769	0.828	0.0122
KCNK1	48	358	297	0.830	0.3862
GOLPH3	51	9541	7935	0.832	0.0034
KCNA1	52	615	512	0.833	0.2305
RRBP1	68	202780	171544	0.846	0.0036
COPA	85	59451	50889	0.856	0.0009
CACNG8	92	15978	13761	0.861	0.0140
COPB2	105	39724	34560	0.870	0.0012
ATP1B1	115	218306	190967	0.875	0.0312
CACNA2D3	155	13210	11738	0.889	0.0423
SEC31A	158	59515	52917	0.889	0.0384
CLCN6	167	1459	1300	0.891	0.1149
GLG1	186	96114	86192	0.897	0.0091
KCNAB2	196	9004	8095	0.899	0.1638
COPG1	323	24042	22085	0.919	0.0009
ATP1A1	410	222599	206605	0.928	0.1087
NTRK3	481	5720	5348	0.935	0.0897
NTRK2	497	17982	16839	0.936	0.0921
SEC16A	685	19259	18319	0.951	0.0184
SAR1A	4230	24186	27889	1.153	0.0744
IGFBP7	4329	2550	6288	2.466	0.0001

Supplemental Table 2

Table S2. Primers used for PCR

Gene cloned	Primers for cloning
MEA6-Flox	5’-GACACTTGACCCCTCCTCTCC-3’ (F)
	5’-AACGGCTCATGCTTGCTAACC-3’ (R)
Cre	5’-CGATGCAACGAGTGATGAGG-3’ (F)
	5’-GCATTGCTGTCACTTGGTCGT-3’ (R)
Thy-GFPm	5’-AAGTTCATCTGCACCACCG-3’ (F)
	5’-TCCTTGAAGAAGATGGTGCG-3’ (R)
MEA6 transgene	5’-AGTCGCTCTGAGTTGTTATCAG-3’ (Rosa-F)
	5’-TGAGCATGTCTTTAATCTACCTCGATG-3’ (Rosa-R)
	5’-AGTCCCTATTGGCGTTACTATGG-3’ (Rosa-Mut-R)
MEA6-splice1	5’-CGAGGCTTCCGATCAATTCGA-3’ (F)
	5’-ATCAGCCATCAGCTCGTCTT-3’ (R)
MEA6-splice2	5’-CTGAAACAGAGTTTAAATTTGAAC-3’ (F)
	5’-GTGGCGGATGGGCTGTCATCC-3’ (R)
Mia2	5’-TGATTTCCGATTCTCCAGTGAG-3’ (F)
	5’-CAAACCATCCTTGCCTTTCTG-3’ (R)
MEA6	5’-CGTTGGAATTGGCAGTATGTG-3’ (F)
	5’-TCTCCCCACATAAAATCGGC-3’ (R)
TALI	5’-TGATTTCCGATTCTCCAGTGAG-3’ (F)
	5’-TCTCCCCACATAAAATCGGC-3’ (R)
Genes analyzed in Real-time PCR	Primers for Real-time PCR
MEA6	5’-TTGGACATGAAGAGTGGCCTAGA-3’ (F)
	5’-AAGCGCCCTTTGGCTGAT-3’ (R)
GAPDH	5’-TGATGACATCAAGAAGGTGGTGAAG-3’ (F)
	5’-TCCTTGGAGGCCATGTAGGCCAT-3’ (R)
Actin	5’-AGGGAAATCGTGCGTGAC-3’ (F)
	5’-GATAGTGATGACCTGACCGT-3’ (R)
SEC31a	5’-CAGTCCTCACTTACGCTAAACC-3’ (F)
	5’-ATTCCCTGCACAGATGTAGCA-3’ (R)
Bip	5’-ACCCTTACTCGGGCCAAATT-3’ (F)
	5’-AGAGCGGAACAGGTCCATGT-3’ (R)
c-Fos	5’-CAAAGTAGAGCAGCTATCTCC-3’ (F)
	5’-CTCATCTTCAAGTTGATCTGT-3’ (R)
Cpg15	5’-CGCGGTGCAAATAGCTTAC-3’ (F)
	5’-TATCTTTCGCCCCTTCCTG-3’ (R)

Reference

1. He LJ, *et al.* (2014) Conditional deletion of Mecp2 in parvalbumin-expressing GABAergic cells results in the absence of critical period plasticity. *Nat Commun* 5:5036.
2. Wang Y, *et al.* (2016) Mea6 controls VLDL transport through the coordinated regulation of COPII assembly. *Cell Res* 26(7):787-804.
3. Lam SM, *et al.* (2014) Extensive characterization of human tear fluid collected using different techniques unravels the presence of novel lipid amphiphiles. *Journal of lipid research* 55(2):289-298.
4. Lam SM, *et al.* (2014) Brain lipidomes of subcortical ischemic vascular dementia and mixed dementia. *Neurobiology of aging* 35(10):2369-2381.
5. Zhang H, *et al.* (2016) Brain-specific Crmp2 deletion leads to neuronal development deficits and behavioural impairments in mice. *Nat Commun* 7.